ARTICLE NO. 80-4108

Three-Layer Interactive Method for Computing Supersonic Laminar Separated Flows

Julius Brandeis* and Josef Rom†
Technion—Israel Institute of Technology, Haifa, Israel

An interactive model for numerical computation of complicated two-dimensional flowfields including regions of reversed flow is proposed. The present approach is one of dividing the flowfield into three regions, in each of which a simplified mathematical model is applied: 1) outer, supersonic flow for which the full potential equation (hyperbolic) is used; 2) viscous, laminar layer in which the compressible boundary-layer model (parabolic) is used; 3) recirculating flow modeled by the incompressible Navier-Stokes equations (elliptic). For matching of the numerical solutions in the three layers, two interaction models are developed: one for pressure interaction, the other for interaction between the shear layer and the recirculating flow. The uniform solution for the whole flowfield is then obtained by iteration of the local solutions under the constraints imposed by matching. The three-layer interactive model is used for solution of the flowfield past an asymmetric cavity. The method is shown to be capable of dealing with backflow without encountering problems at separation, characteristic to the boundary-layer approach. Successful matching of flow variables u, v, and $\partial u/\partial y$ along the matching boundary of the cavity is demonstrated and there is no need to fix the stagnation point as was the case in some previous researches. However, a constraint on downstream pressure had to be imposed in order to achieve convergence.

Nomenclature

AR = aspect ratio, $= H/L$
a = speed of sound ($a=\sqrt{\gamma RT}$)
c_p = specific heat at constant pressure
c_v = specific heat at constant volume
H = height of the cavity
k = thermal conductivity
L = characteristic length
M = Mach number ($M=u/a$)
Pr = Prandtl number ($Pr=\mu c_p/k$)
p = pressure
R = constant in perfect gas law
Re = Reynolds number ($Re=\rho UL/\mu$)
S = slope of the matching streamline
T = temperature
t = time
U = freestream velocity vector
u = velocity component in the x direction
v = velocity component in the y direction
x = Cartesian coordinate parallel to the plate
y = Cartesian coordinate normal to the plate
γ = ratio of specific heats ($\gamma=c_p/c_v$)
Δ = small increment, difference
δ^* = displacement thickness of the boundary layer
δ = matching thickness (height to the matching streamline)
ζ = vorticity function
η = upward-running characteristic
θ = streamline angle
μ = viscosity coefficient in the boundary-layer equations
ν = Prandtl-Meyer function of potential flow
ρ = density
ψ = stream function

Subscripts

BL = boundary-layer calculation
C = cavity calculation
e = local outer flow condition
r = "round" number
∞ = reference to undisturbed flow

Received Oct. 6, 1979; revision received March 18, 1980.

Index categories: Boundary Layers and Convective Heat Transfer—Laminar; Computational Methods; Jets, Wakes, and Viscid-Inviscid Flow Interactions.

*Graduate Instructor, Dept. of Aeronautical Engineering (presently NRC Associate at NASA Ames Research Center, Moffett Field, Calif.). Member AIAA.

†Professor, Lady Davis Chair in Experimental Aerodynamics, Dept. of Aeronautical Engineering. Member AIAA.

Introduction

INTERACTIVE, multilayer methods for which a specialized model is adopted for each layer present an alternative to using the general Navier-Stokes equations for the entire flowfield. The advantages inherent in using an interactive approach based upon boundary-layer simplification in the region where viscous forces are important are as follows: 1) shorter computer processing time as well as smaller core requirements than for the Navier Stokes methods, 2) no Reynolds number limitations for the field, and 3) no need to specify the outflow condition.

On the other hand, formulation of an interaction model involves problems associated with convergence and stability of multicomponent solutions. Another inherent limitation centers around the approximate nature of interactive methods, giving rise to problems such as breakdown of the solution in the vicinity of the separation point. This singular behavior of solution of boundary-layer equations near separation has been given wide attention in recent years (e.g., by Stewartson[1]). There have been several successful attempts to continue the interactive, numerical solution of the boundary-layer equations into the region of reversal flow. Thus, Werle and Vatsa[2] used the alternating direction implicit (ADI) numerical scheme, while Williams[3] applied the downstream-upstream integration technique (DUIT) for the backflow. Both these techniques require special treatment of the region around the separation point, as does the method of Catherall and Mangler,[4] who specify the displacement thickness distribution in the vicinity of separation, thus obtaining regular behavior of solution there. Regular behavior of the solution to the boundary-layer equations is in general achievable through the use of inverse methods (e.g.,

Ref. 5), in which displacement thickness or wall shear is specified.

It is felt that for the present the most promising method for dealing with recirculation is to treat that part of the flowfield as a self-contained region in which an appropriate mathematical model specialized for this purpose is used. With that in mind, an interactive model for computation of complicated flowfields including the extensive region of recirculation is proposed. The method consists of three layers: the outer, supersonic flow, described by the exact potential equation together with the irrotationality relation; the shear layer modeled by the laminar, compressible boundary-layer equations; and a region containing all of the reversed flow, in which the incompressible Navier-Stokes model is used. (A similar model, using a linearized treatment of the shear layer was applied by Weiss[6] for the solution of the hypersonic near-wake problem.)

The matching procedures in the present method utilize the streamline displacement-pressure approach for the pressure interaction, and a new overlapping regions approach for the shear layer/recirculating flow interaction. These, together with the Navier-Stokes treatment of the backflow, resulted in regular behavior of solution even at the separation and reattachment points.

In this approach the interactive model is applied to supersonic viscous flow over an asymmetric cavity. The flow is assumed to be laminar as well as two-dimensional. Steady-state equations are used for the shear layer, although cavity flows tend in practice to exhibit a varying degree of periodicity. The numerical model should be applicable as well for computation of turbulent flow if use is made of the eddy viscosity concept in the viscous region.

Mathematical Formulation of Flow in Three Layers

In the outermost region of potential flow, the exact equations of motion, assuming irrotationality, are

$$(u^2-a^2)\frac{\partial u}{\partial x}+uv\left(\frac{\partial u}{\partial y}+\frac{\partial v}{\partial x}\right)+(v^2-a^2)\frac{\partial v}{\partial y}=0 \tag{1}$$

$$\frac{\partial u}{\partial y}-\frac{\partial v}{\partial x}=0 \tag{2}$$

with a defined as the speed of sound.

Solutions to Eq. (1) are conveniently computed for the supersonic flow using the method of two-family characteristics. Such full treatment of the potential region was pointed out by Miller[7] to be a prerequisite for a well-posed interaction problem. In the present work, the main function of the solution of the outer flow is to compute the correct interaction pressure along the common boundary with the viscous flow. Thus, no attempt has been made to account for shocks, as these are not expected to appear in the present problem in a region affecting the pressure solution along the matching boundary.

Below the potential region there exists a viscous, compressible transition layer bounded from below by either a solid wall or by fluid interphase with a region of slowly recirculating flow. It is assumed that this layer is relatively thin, and therefore that the boundary-layer approximation can be used in this region. The governing equations, nondimensionalized by the freestream reference values are:

Boundary layer:

$$\rho u\frac{\partial u}{\partial x}+\rho v\frac{\partial u}{\partial y}=-\frac{dp}{dx}+\frac{1}{Re}\frac{\partial}{\partial y}\left(\mu\frac{\partial u}{\partial y}\right) \tag{3}$$

$$\rho u\frac{\partial T}{\partial x}+\rho v\frac{\partial T}{\partial y}=u\frac{dp}{dx}+\frac{1}{Re\,Pr}\frac{\partial}{\partial y}\left(\mu\frac{\partial T}{\partial y}\right)+\frac{\mu}{Re}\left(\frac{\partial u}{\partial y}\right)^2 \tag{4}$$

Continuity:

$$\frac{\partial(\rho u)}{\partial x}+\frac{\partial(\rho v)}{\partial y}=0 \tag{5}$$

State:

$$p=\frac{\gamma-1}{\gamma}\rho T \tag{6}$$

Viscosity:

$$\mu=[(\gamma-1)M_0^2]^{0.76}T^{0.76} \tag{7}$$

together with the boundary conditions on u, v, and T at the lower boundary, and the outer edge compatibility relations

$$\rho_e u_e\frac{\partial u_e}{\partial x}=-\frac{dp}{dx} \tag{8}$$

$$\rho_e u_e\frac{\partial T_e}{\partial x}=u_e\frac{dp}{dx} \tag{9}$$

Equations (3-7) together with the boundary conditions are solved downstream from the initial station. The computational region is taken to extend in the lateral direction high enough so that the velocity and temperature gradients $\partial u/\partial y$ and $\partial T/\partial y$ can be neglected at the outer boundary.

The solution of the mathematical problem is obtained through the use of Reyhner's method[8] by replacing the nonlinear partial differential equations with a set of linear difference equations. The solution obtained at each step from the linear difference equations is used to calculate an improved solution at that step through iteration, until the difference between flow variables for two successive iterations is as small as desired.

The recirculating flow is contained in the present case by a rectangular cavity bounded on three sides by no-slip walls. Along the fourth, open boundary, the flow merges with the shear layer which through the action of viscous stresses provides the driving force for the recirculation. For small cavities ($L\sim H\sim 0(\delta)$) the anticipated recirculating velocities are in the low subsonic range for moderate supersonic Mach numbers in the outer flow. Consequently computation of the cavity flow is carried out with the incompressible Navier-Stokes equations. As a further consequence of the low recirculation velocities, the density and velocity fields are assumed to be only weakly coupled, and the energy equation is not considered at the present stage.

Incompressible Navier-Stokes equations written in the vorticity-stream function form and normalized by cavity length (L_c), typical velocity (U_c) and characteristic density and viscosity are

$$\frac{\partial\zeta}{\partial t}=-u\frac{\partial\zeta}{\partial x}-v\frac{\partial\zeta}{\partial y}+\frac{1}{Re}\nabla^2\zeta \tag{10}$$

$$\frac{\partial\psi}{\partial t'}=\nabla^2\psi-\zeta \tag{11}$$

t' in Eq. (11) can be regarded as a nonphysical iteration time. Only the converged result (steady state) is of interest. The boundary conditions at the three no-slip walls are

$$\psi=0$$

$$\zeta=\partial^2\psi/\partial y^2 \text{ along horizontal wall}$$

$$\zeta=\partial^2\psi/\partial x^2 \text{ along vertical walls}$$

ψ and ζ along the fluid interphase boundary will be discussed later, together with the matching method.

Equations (10) and (11) are discretized using the fully explicit, second-order accurate forward time-center space (FTCS) numerical scheme. Although the Reynolds number limit for stability associated with this approach is only somewhat higher than 100, it was sufficiently high for the small cavities considered in this study.

Formulation of Interaction between Three Layers

The equations of motion for each of the three layers must now be solved interactively under the condition that the solutions in any two adjacent regions be compatible across the common boundary.

Viscous/Inviscid Interaction

For interaction of the viscous layer with the potential flow, the pressure and the flow direction need to be matched. The matching is to be carried out along one of the outer streamlines of the shear layer. Specific choice of the streamline for which $u/U_\infty = 0.98$ nominally was made in observance of the fact that the flow above is already nearly isentropic ($\partial T/\partial y \sim \partial u/\partial y \sim \partial \rho/\partial y \simeq 0$). Choice of a higher streamline would carry with it a larger error due to neglecting the $\partial p/\partial y$ term, while adding little to the accuracy of the results.

The interaction procedure involves matching pressure p and streamline slope S iteratively at each x station before advancing downstream. The actual iteration scheme adopted here is similar to that proposed by Brune et al.[9] However, the present method avoids the need for linearization of complicated sets of equations involved in Ref. 9. Convergence path diagram involving the p-δ plane (where δ is defined as the height of the matching streamline, termed matching thickness) for the present method appears in Fig. 1. Briefly, on the basis of an initial guess of δ both the outer and the shear layer flows are solved. Using an empirical constant to speed up convergence, a new δ is computed and both sets of equations are solved, locating the second iteration values of δ and p. The initial third iteration value of p is obtained by linear interpolation or extrapolation from the values of p and δ obtained from the first two iterations. Corresponding outer flow Mach number and Prandtl-Meyer angle ν are computed from

$$M_3 = \sqrt{\frac{2}{\gamma-1}\left[\frac{1+\frac{\gamma-1}{2}M_2^2}{\left(\frac{p_3}{p_2}\right)^{\frac{\gamma-1}{\gamma}}} - 1\right]} \tag{12}$$

and

$$\nu_3 = \sqrt{\frac{\gamma+1}{\gamma-1}}\tan^{-1}\sqrt{\frac{\gamma-1}{\gamma+1}}\sqrt{M_3^2-1} - \tan^{-1}\sqrt{M_3^2-1} \tag{13}$$

Using Eqs. (12) and (13), θ is found from the relation $\theta = \nu + \sin^{-1}(1/M)$. Now, the final values of p and δ for the third iteration are obtained from the solutions in the two layers. The procedure is repeated until the difference in successive values of δ is acceptably small.

It is to be noted that for the case of subcritical boundary layer, the interaction constitutes a boundary value problem[10,11] and therefore the upstream boundary condition must be carefully chosen in order for the solution to exhibit desired downstream behavior.

Shear Layer/Recirculating Flow Interaction

It is recalled that in formulation of the mathematical models for the shear layer and the recirculating flow, two different sets of normalization factors were used. Consequently, two different scales are inherent in the interaction. (Multiple scaling arising in interactive solutions has been discussed by Rom.[12])

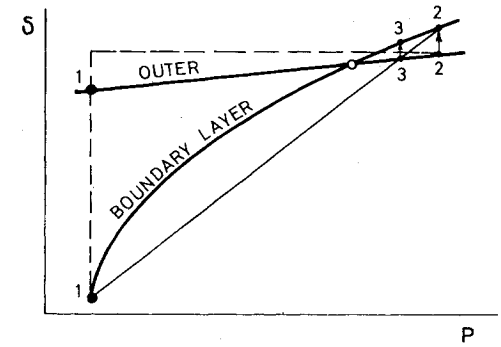

Fig. 1 Convergence path for the present method.

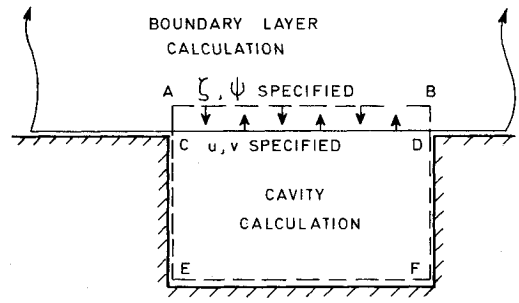

Fig. 2 Schematic of two regions used for interactive cavity/boundary layer computation.

The geometry of the matching model adopted in this work is illustrated in Fig. 2. The important, innovative feature of this model is the overlap region ABCD between the domains of shear layer and recirculating flow computation. There are now seen to be two matching boundaries, AB, and CD, defining the matching region in which the flow undergoes "transition" between the two fields of computation.

The upper matching line AB lies within the region where flow is calculated by the boundary-layer equations. It is also the upper boundary for the Navier-Stokes calculation of the cavity flow inside the rectangle ABFE. Vorticity ζ and stream function ψ boundary conditions are then calculated within the shear layer using

$$\zeta = \frac{\partial u}{\partial y} - \frac{\partial v}{\partial x} \tag{14}$$

$$\frac{\partial^2 \psi}{\partial x^2} = -\frac{\partial v}{\partial x} \tag{15}$$

The lower matching line CD is analogously seen to lie within the Navier-Stokes computation region, from which, then, the velocities u and v are calculated and supplied as boundary conditions for the shear layer computation. Each time that boundary conditions are exchanged between the regions, their scaling has to be adjusted accordingly.

The height of the overlap region is taken here as one grid interval in the transverse direction though it need not be restricted as such. One criterion which has to be considered in adjusting the height of the overlap region is the validity of the incompressibility assumption for the flows within the cavity.

The interactive computation of the shear layer and recirculating flow is carried out iteratively. However, since now the joint solution of parabolic and elliptic equations is considered, the approach must be different from the one

utilized in matching the shear layer with the outer flow. Consequently, the shear layer solution is marched across the span of the cavity and only then is the recirculating flow computed using the available boundary conditions. The cycle is repeated by solving the shear layer equations once more across the cavity, but with updated boundary conditions. The process is continued until the maximum difference between flow variables for two successive cycles is acceptably small.

It is noteworthy that the present method does not require that the locations of stagnation points (separation and reattachment) be supplied. These are obtained from the results of the calculation as part of the iterative solution. A more detailed description of this method, including convergence characteristics is presented by Brandeis.[13]

Interactive Solution of Whole Field

The solution cycle used for the three-field flow computation is illustrated by the schematic and flow diagram in Fig. 3. The problem was divided into two parts, with the shear layer emerging as the pivotal element of the interaction: 1) interactive computation of the outer flow and the shear layer, which fixes the interaction pressure; and 2) interactive computation of the shear layer and the recirculating flow, which establishes the shape of the velocity profiles in the region where the two flows merge. The two parts are mutually dependent and the coupling is accomplished once more through iteration.

It was found convenient to work with two different streamwise step sizes in the two parts of the problem. The smaller increment, $\Delta x/L_{BL}=0.001$ (L_{BL} is the distance from the leading edge of the plate to the beginning of the interaction), was used for the shear layer recirculating flow computation in order to give reasonable resolution within the cavity. The larger, $\Delta x/L_{BL}=0.003$, was used for the interaction with the outer flow in the order to cut down on the number of steps needed to span the cavity. This was not felt to be overly coarse for the case of a cavity with L_c of the order δ considered here.

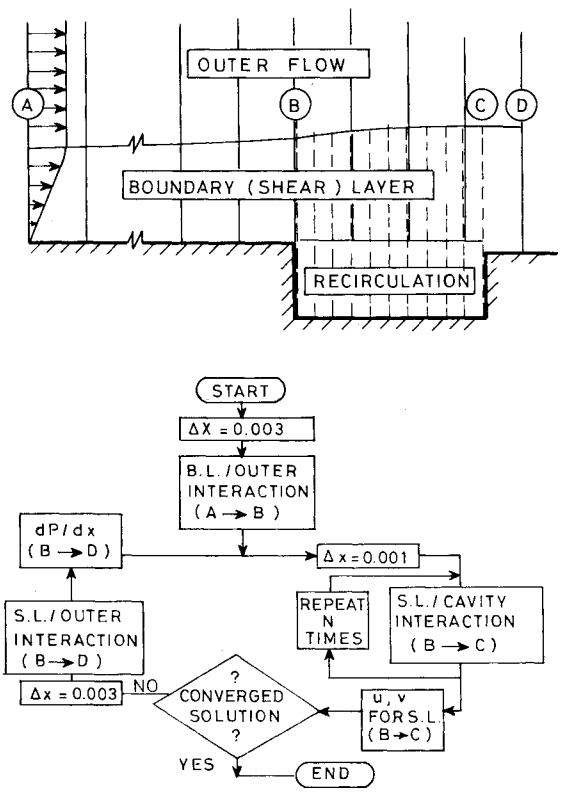

Fig. 3 Schematic and flow diagram for three-layer flow computation.

The three-field interactive solution is initiated at the leading edge of the cavity (point B in Fig. 3) based upon the results of the interactive boundary layer/potential flow computation carried out between points A and B.

Starting at point B and continuing until point C, the shear layer/recirculating flow problem was solved N times (N was taken as 2 or 3) for the outer flow pressure distribution supplied (initially taken as uniform). For this solution the u and v velocity distributions along the matching boundary constituting the extension of the flat plate were prescribed as the lower boundary conditions for the shear layer. With these conditions the shear layer was computed interactively with the outer flow using the coarser x step size, ending the first cycle (called round). The pressure distribution obtained was prescribed as the outer pressure distribution at the beginning of the next round, and the solution was continued until reasonable convergence was reached for all three fields.

Convergence of Interactive Solution

The question of convergence of the three-field solution presents a special problem, in that updating the matching between any two regions may have an adverse effect on the matching previously executed with the third layer. It is therefore necessary to develop a procedure insuring the convergence of the complete interaction problem.

The main variables which have to be monitored in order to insure convergence are p, obtained along the span from the pressure interaction, and u and v along the interphase between the shear layer and the recirculating flow obtained from the interaction between these two layers. The overall solution will in general proceed toward convergence if the differences in pressure and in the two velocity components along the cavity's fluid interphase decrease for consecutive rounds. It is sought to modify the pressure distribution used for executing the shear layer/recirculating flow matching with the goal of minimizing the anticipated error in u and v along the interphase. This can be accomplished by examining the values of p, u, and v from the previous two rounds. (It is to be recalled that each round starts with the shear layer/recirculating flow interaction.) Then using the definitions

$$\Delta u_{r-1}=u_{r-1}-u_{r-2}$$

$$\Delta u_{r-2}=u_{r-2}-u_{r-3}$$

$$\Delta v_{r-1}=v_{r-1}-v_{r-2}$$

$$\Delta v_{r-2}=v_{r-2}-v_{r-3}$$

where r identifies the "round number," the pressure used for initiating the new round is interpolated

$$p_r=\frac{1}{2}\left[\frac{P_{r-1}\Delta u_{r-2}-P_{r-2}\Delta u_{r-1}}{\Delta u_{r-2}-\Delta u_{r-1}}+\frac{P_{r-1}\Delta v_{r-2}-p_{r-2}\Delta v_{r-1}}{\Delta v_{r-2}-\Delta v_{r-1}}\right] \tag{16}$$

This calculation is made for each x station across the span of the cavity.

Because of the boundary value nature of the pressure interaction formulation, it is necessary to make periodic adjustments of the matching streamline's slope at the first interactive step, in order to satisfy the selected downstream boundary condition. This is accomplished through repeated streamwise passes of the solution.

Convergence of the solution is said to be reached when the maximum difference between the values of the variables for two consecutive rounds is smaller than some preselected value. Usually the behavior of the key variables along the matching lines provides a satisfactory criterion for convergence, as the relative convergence errors at the matching boundaries tend to be greater than anywhere else in the field.

Application of Asymmetric Cavity

The three-layer interactive method is now applied to the test problem of a rectangular, asymmetric cavity of aspect ratio 0.4, whose reattachment face is taken as 0.9 the height of the separation face (see Fig. 3a). The span of the cavity is 0.01 the length of the flat plate preceeding the cavity ($L_c/L_{BL}=0.01$), which is of the order of the boundary-layer thickness at the start of the interaction.

The flow conditions adopted for the present solution are: $M_\infty=2.25$, $Pr=1$, $Re_{BL}=10^5$, $Re_c=5.4$ with $\partial T/\partial y=0$, the adiabatic wall assumption, used in the viscous layer.

The shear layer/outer flow interaction is carried out with a streamwise step size $\Delta x/L_{BL}$ of 0.003, for the total of 5 steps across the span of the cavity, while for the interaction of the shear layer with recirculating flow $\Delta x/L_{BL}=0.001$ is used, yielding 11 computational steps across the cavity. The lateral extent of the computational regions is taken as 81 grid points for the outer flow, 100 for the shear layer, and 12 for the recirculating flow.

As discussed previously, a downstream compatibility condition needs to be satisfied for a well-posed pressure interaction problem. Some researchers[2,8] have used $dp/dx=0$ or $d^2p/dx^2=0$ as the downstream condition. In the present work, the pressure at the last interactive station is held at a fixed value. This station, labeled D in Fig. 3, falls downstream of the cavity's trailing edge. Although more restrictive than the above-mentioned conditions, keeping the downstream pressure fixed had the desirable stabilizing effect on the reversed flow computation. The downstream pressure was taken as 0.12933 ($P_\infty=0.1410$) as computed during the first round. It is therefore a result of letting the potential stream flow over the outer streamline of the shear layer, located from the first iteration of the shear layer/cavity flowfield.

The boundary-layer calculation at the downstream-most station was initiated one grid point above the solid wall, as necessitated by lowering the step-up side of the cavity. The boundary conditions u and v were assigned at this station by extrapolation. The corresponding outflow conditions for the Navier-Stokes computation was found by interpolating, using the three neighboring grid points: above, below, and upstream.

For the present case, upstream influence was not taken into account. The iterative solution of the three layers was initiated from a previously computed profile at the cavity's leading edge.

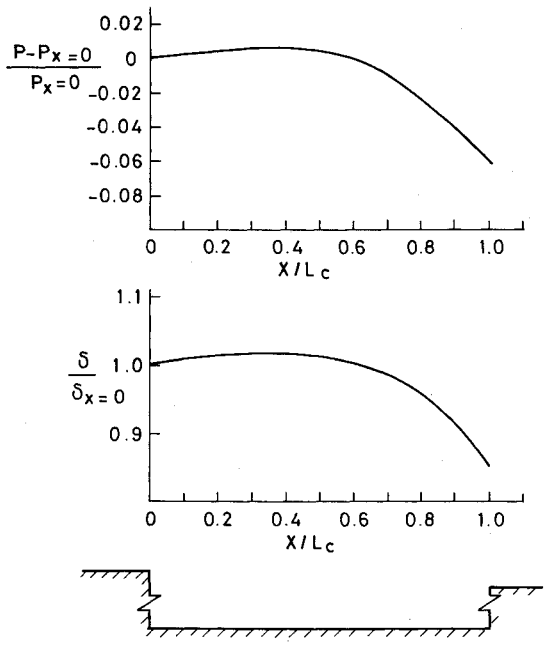

Fig. 4 Pressure and matching thickness variation along the cavity's span: $AR=0.4$, $Re_c=5.4$, $Re_{BL}=10^5$, $Pr=1$, $M_\infty=2.25$.

Results of the three-field interactive solution to the problem described in this section, subject to the assumptions just listed, appear in Figs. 4-10. It should be recalled that at this stage these results are meant primarily to demonstrate the feasibility of carrying out interactive three-layer computation, and not necessarily to constitute an accurate solution to the field.

Figure 4 shows the variation of the outer pressure and matching thickness δ along the span of the cavity. Both distributions show a rise over the first half of the span, followed by a sharper fall over the second half. This fall is due to the assumption of the downstream pressure. The experimental results of Charwat et al.[14] show that for small symmetric cavities for which $\delta^*/H_c=0(1)$ and $AR\leq 5$, the cavity pressure is somewhat higher than the freestream as the shear layer thickens across the cavity's span, causing an upward displacement of the outer flow. The interactive computation did exhibit this trend of pressure rise over the first half-span of the cavity. The present condition of lower pressure at the trailing edge was thought justifiable in view of the lowering of the step-up wall of the cavity, but the precise value may need adjustment for accuracy.

Figures 5-9 aim at examining the effects of pressure interaction on the structure of the flow within the cavity and in the interphase with the shear layer.

Upon examining the distribution of u and v velocity components along the horizontal matching boundary passing through the downstream corner of the cavity (CD on Figs. 5 and 6), a tendency to form a plateau for both velocity components is observed over the initial half of the length scale. This is due to pressure interaction, as the corresponding results with $dp/dx=0$ show smooth variation of u and v. The subsequent rise in the u velocity is due to the turning of the flow inward in order to reattach on the lowered surface downstream of the cavity. The magnitude of the u velocity in the plateau regions is rather low (about 2% of U_e) but this seems to be due to geometry.

Figure 6 indicates an increase in length of about 30% L_c of the region in which the shear layer scavenges mass from the recirculating flow at the expense of the region in which that mass is reinjected into the cavity, caused by the pressure interaction. This fact points to a downstream shift of the vortex's center caused by the streamwise pressure gradient. This is clearly seen to be the case in Fig. 7 which shows the stream function contour map of the cavity flow with and without pressure interaction. The vortex is also seen to be somewhat askew (its axes having rotated clockwise about 10 deg) as a result of asymmetric geometry.

Figure 8 shows the vorticity contour map and lends further support to what has been said until now about the vortex structure. Worthy of noting is the large gradient of vorticity in the vicinity of the downstream wall resulting from external pressure variation.

A graph of pressure variation along the solid walls of the cavity appears in Fig. 9. These pressures were computed by solving the momentum equations for pressure along no-slip walls which result in

$$p=\int_0^{L_c}\frac{1}{Re}\frac{\partial\zeta}{\partial y}dx+\text{const} \tag{17}$$

$$p=-\int_{y_1}^{y_2}\frac{1}{Re}\frac{\partial\zeta}{\partial x}dy+\text{const} \tag{18}$$

along the horizontal and vertical walls, respectively. The results show a slight drop in pressure along the upstream vertical wall, a 1% rise over the second half of the bottom surface, followed by a much sharper rise (to 3%) along the

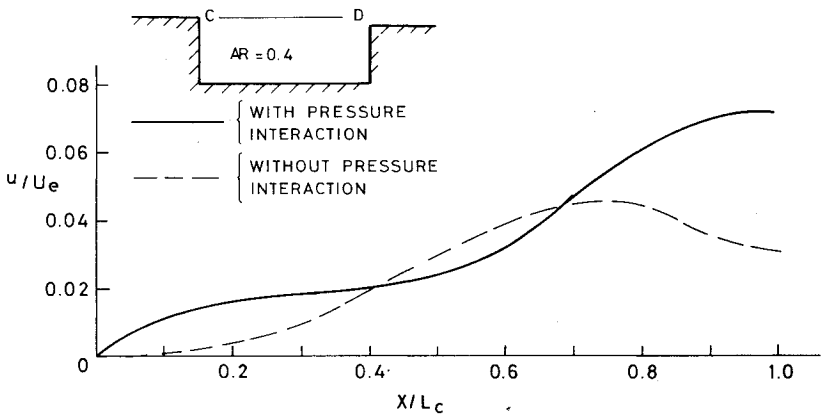

Fig. 5 u **velocity distributions along the upper bound of the cavity:** $\mathcal{R}=0.4$, $Re_c=5.4$, $Re_{BL}=10^5$, $Pr=1$, $M_\infty=2.25$.

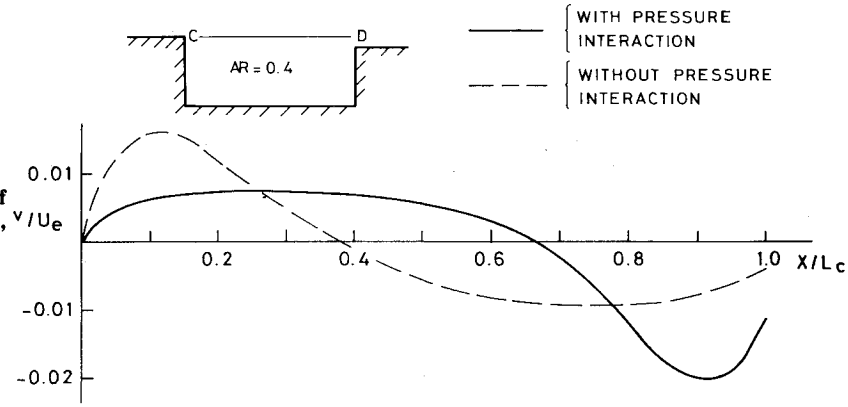

Fig. 6 v **velocity distribution along the upper bound of the cavity:** $\mathcal{R}=0.4$, $Re_c=5.4$, $Re_{BL}=10^5$, $Pr=1$, $M_\infty=2.25$.

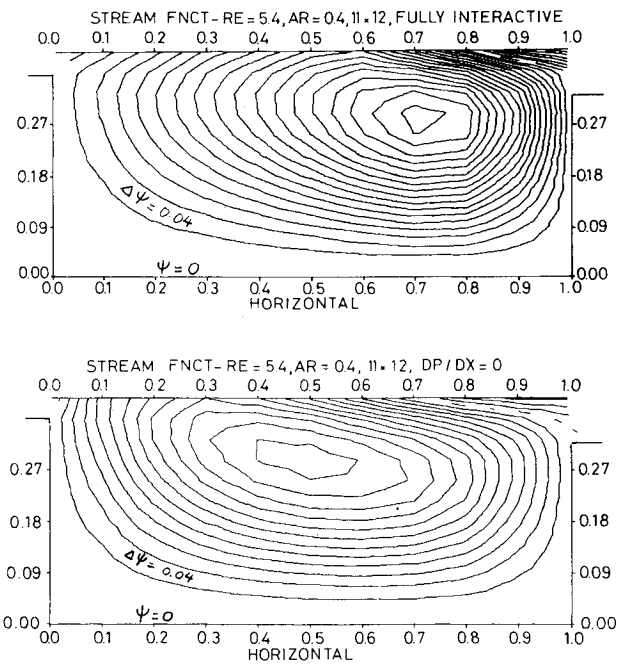

Fig. 7 Stream function contour map for the cavity: $\mathcal{R}=0.4$, $Re_c=5.4$, $Re_{BL}=10^5$, $Pr=1$, $M_\infty=2.25$.

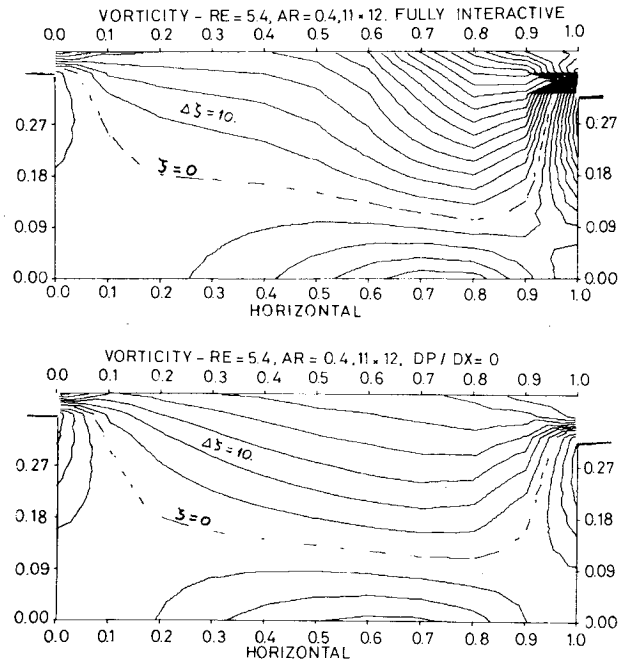

Fig. 8 Vorticity contour map for the cavity: $\mathcal{R}=0.4$, $Re_c=5.4$, $Re_{BL}=10^5$, $Pr=1$, $M_\infty=2.25$.

downstream wall. These findings are consistent with the results of Ref. 14 although smaller in magnitude. (Reference 14 considered turbulent shear layer and different geometry. The Reynolds number was also about 15 times greater than in the present case. For these reasons no quantitative comparison can be attempted.) The difference between pressure results for interactive and noninteractive calculations is seen to be small except on the downstream wall, where it reaches about 50%. This comparison can also be made from examination of the vorticity contour map in Fig. 8.

Finally, Fig. 10 shows the development of the recirculating flow/shear layer u velocity profile at several spanwise stations of the cavity. The bulging out of the profile at the downstream corner is due to the pressure drop caused by the lowered wall. The smooth matching of the u velocity between the two regions is also evident in Fig. 10. In actuality, the

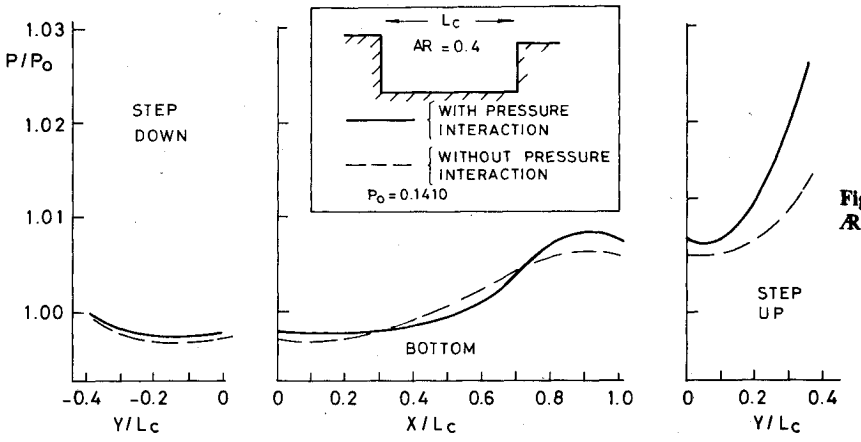

Fig. 9 Pressure variation along the cavity's solid walls: $\bar{R}=0.4$, $Re_c=5.4$, $Re_{BL}=10^5$, $Pr=1$, $M_\infty=2.25$.

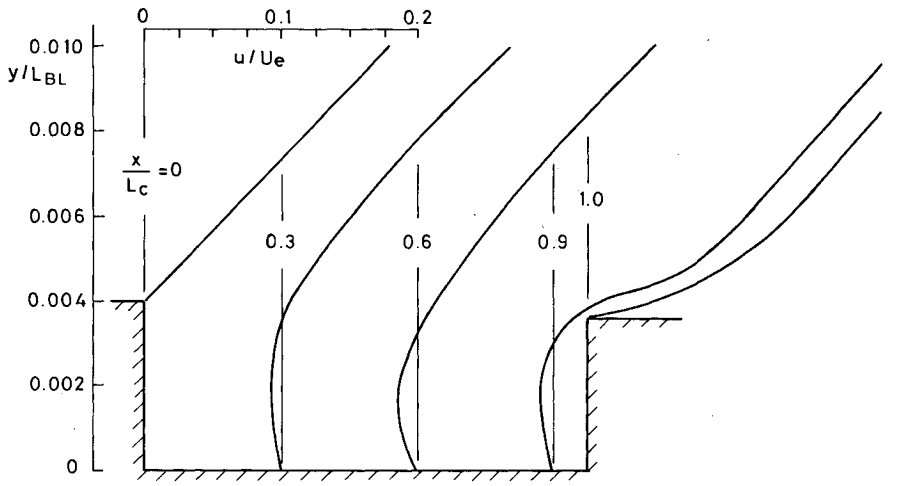

Fig. 10 Variation of u velocity profile in the shear layer/cavity flow: $\bar{R}=0.4$, $Re_c=5.4$, $Re_{BL}=10^5$, $Pr=1$, $M_\infty=2.25$.

interactive method used allows matching of not only u and v but of $\partial u/\partial y$ as well along the cavity shear layer boundary.

The iterative computation was allowed to proceed for 11 rounds (full cycles), which encompassed 23 sweeps (shear layer/cavity interaction cycles). The check of convergence of the three fields was carried out at that stage. The maximum, relative, iterative error in pressure along shear layer's outer (matching) streamline was found to be about 5×10^{-2} times the pressure drop along the cavity.

Within the recirculating flow region the maximum convergence errors were greater—approaching 10^{-1} in the vorticity and stream function fields. When the two parts of the problem was considered separately, convergence to within an error of 5×10^{-6} was obtained with 3-5 iterations per step for the outer flow/shear layer interaction while for the shear layer/cavity flow after 20 sweeps of the field the maximum convergence errors were less than 10^{-2}. Increasing the number of sweeps to 50 resulted in up to two orders of magnitude decrease in the error. These results make clear that better convergence can be obtained by increasing the number of iterations.

The CPU time required for this computation using the field size described was under 8 min on an IBM 370-168 computer.

Conclusions

A three-layer interactive method for computation of complicated two-dimensional, supersonic flowfields was proposed. Within this framework two methods were developed for carrying out matching between the outer flow and the shear layer, and between the shear layer and the recirculating flow. Application was made to flowfield about asymmetric cavity, illustrating the feasibility of the present approach.

At present, a constraint was adopted regarding the downstream pressure in order to facilitate solution. A less restrictive compatibility condition, such as $dp/dx=0$ or $d^2p/dx^2=0$ is feasible with the present method, providing that pressure interaction is continued far enough downstream for such condition to hold true.

The model developed is attractive in that it was designed to deal with the problem of backflow by applying the incompressible Navier-Stokes equation in a limited region of flow reversal. This, then, avoided the difficulties associated with the boundary-layer approach to the problem. The overlapping regions matching methods were shown capable of coupling the local Navier-Stokes solution to that of the shear layer above by matching three flow variables: u, v, and $\partial u/\partial y$. Furthermore, no prior assumption of the stagnation points location was required.

The computing time required for the interactive solution presented was relatively modest—under 8 min on the IBM 370-168 computer.

The extension of the present method to turbulent regime can be made using the interaction models developed in this study by adopting an eddy viscosity model for computation of the shear layer.

Acknowledgment

Part of this work was carried out while the first author was under tenure of the Lady Davis Fellowship at the Technion.

References

Stewartson, K., "Multistructural Boundary Layers on Flat Plates and Related Bodies," *Advances in Applied Mechanics*, Vol. 14, 1974, pp. 145-239.

[2]Werle, M. J. and Vatsa, V. N., "New Method for Supersonic Boundary-Layer Separation," *AIAA Journal*, Vol. 12, Nov. 1974, pp. 1491-1497.

[3]Williams, P. G., "A Reverse Flow Computation in the Theory of Self-Induced Separation," *Proceedings of International Conference on Numerical Methods in Fluid Dynamics*, Twente University of Technology, 1976, *Lecture Notes in Physics*, Vol. 59, pp. 445-451.

[4]Catherall, D. and Mangler, K. W., "The Integration of the Two-Dimensional Laminar Boundary Layer Equations Past the Point of Vanishing Skin Friction," *Journal of Fluid Mechanics*, Vol. 26, Sept. 1966, pp. 163-182.

[5]Carter, J. E., "Solutions for Laminar Boundary Layers with Separation and Reattachment," AIAA Paper 74-583, Palo Alto, Calif., June 1974.

[6]Weiss, R. F., "A New Theoretical Solution of the Laminar, Hypersonic Near Wake," *AIAA Journal*, Vol. 5, Dec. 1967, pp. 2142-2148.

[7]Miller, G., "Mathematical Formulation of Viscous-Inviscid Interaction Problems in Supersonic Flow," *AIAA Journal*, Vol. 11, July 1973, pp. 938-942.

[8]Reyhner, T. A. and Flugge-Lotz, I., "The Interaction of Shock Wave with a Laminar Boundary Layer," *International Journal of Non-Linear Mechanics*, Vol. 3, 1968, pp. 173-199.

[9]Brune, G. W., Rubbert, P. E., and Nark, T. C., Jr., "A New Approach to Inviscid Flow/Boundary Layer Matching," AIAA Paper 74-601, Palo Alto, Calif., June 1974.

[10]Garvine, R. W., "Upstream Influence in Viscous Interaction Problems," *The Physics of Fluids*, Vol. 11, July 1968, pp. 1413-1423.

[11]Baum, E., "An Interaction Model of a Supersonic Laminar Boundary-Layer on Sharp and Rounded Backward Facing Steps," *AIAA Journal*, Vol. 6, March 1968, pp. 440-447.

[12]Rom, J., "Flows with Strong Interaction Between the Viscous and Inviscid Regions," *SIAM Journal of Applied Mechanics*, Vol. 29, No. 2, Sept. 1975, 309-328.

[13]Brandeis, J., "Computation of Supersonic Two-Dimensional Viscous Flows Using Multilayer Interactive Method," D.Sc. Thesis, Technion-Israel Institute of Technology, Dept. of Aeronautical Engineering, Haifa, April 1979.

[14]Charwat, A. F., Roos, J. N., Dewey, F. C., Jr., and Hitz, J. A., "An Investigation of Separated Flows—Part I: The Pressure Field," *Journal of Aeronautical Sciences*, Vol. 28, June 1961, pp. 457-470.